

# Analytic structure of solutions of the one-dimensional Burgers equation with modified dissipation

Walter Pauls<sup>1,2</sup> and Samriddhi Sankar Ray<sup>3</sup> ‡

<sup>1</sup>Max-Planck-Institut für Dynamik und Selbstorganisation, Am Faßberg 11, 37073 Göttingen, Germany

<sup>2</sup>Mühlweg 4, 73460 Hüttlingen, Germany

<sup>3</sup>International Centre for Theoretical Sciences, Tata Institute of Fundamental Research, Bangalore 560089, India

## Abstract.

We use the one-dimensional Burgers equation to illustrate the effect of replacing the standard Laplacian dissipation term by a more general function of the Laplacian – of which hyperviscosity is the best known example – in equations of hydrodynamics. We analyze the asymptotic structure of solutions in the Fourier space at very high wave-numbers by introducing an approach applicable to a wide class of hydrodynamical equations whose solutions are calculated in the limit of vanishing Reynolds numbers from algebraic recursion relations involving iterated integrations. We give a detailed analysis of their analytic structure for two different types of dissipation: a hyperviscous and an exponentially growing dissipation term. Our results, obtained in the limit of vanishing Reynolds numbers, are validated by high-precision numerical simulations at non-zero Reynolds numbers. We then study the bottleneck problem, an intermediate asymptotics phenomenon, which in the case of the Burgers equation arises when one uses dissipation terms (such as hyperviscosity) growing faster at high wave-numbers than the standard Laplacian dissipation term. A linearized solution of the well-known boundary layer limit of the Burgers equation involving two numerically determined parameters gives a good description of the bottleneck region.

PACS numbers: 47.27.-i, 82.20.-w, 47.51.+a, 47.55.df

## 1. Introduction

The physics of a fluid in a turbulent state is multiscale. Hence, it is convenient to study turbulence by separating the scales into energy injection  $L$ , inertial  $r$ , and dissipation  $\eta$  ranges [1]. Such a classification has proved useful, both theoretically and numerically, to develop models which mimic such scales. These models have the advantage of being less complex than the original system and hence, more tractable. Indeed, we owe much of our understanding of the physics and mathematics of turbulent flows, validated by experiments, observations and detailed simulations, to such reduced models. The most celebrated example of this is the tremendous advance made within the framework of three-dimensional, homogeneous, isotropic turbulence (in the limit of vanishing kinematic viscosity  $\nu$ ). Such a

‡ Author to whom all correspondence should be addressed.

framework, which ignores the specific details of the forcing and dissipation mechanisms, has yielded several important and universal results [2] for the inertial scale and forms the basis of Kolmogorov's seminal work in 1941 [3]. In particular, the most important results stemming from such a model are those related to 2-point correlation functions, multiscaling, and their universality [2, 4, 5].

Despite the success in understanding the physics of the inertial range, the theoretical underpinnings of the model of homogeneous, isotropic turbulence are largely irrelevant for questions related to the regularity of such flows. This is because these questions – which still rank amongst the most profound and fundamental in mathematics [6, 7] – have answers hidden in the behaviour of flows at scales much smaller than the inertial range. The key to such answers lie in the study of incompressible, three-dimensional Navier-Stokes and Euler equations whose non-linearity encodes information of the velocity field at all scales ranging from the largest to the smallest. Remarkably, the issue of the regularity of solutions (for sufficiently smooth initial conditions) is still not settled [8, 9, 10, 11] even for the viscous Navier-Stokes equation [12, 13, 14, 15]. What is reasonably clear, though, is that for initial conditions which are analytic, periodic functions, solutions to these equations, while remaining analytic, have complex singularities as seen, e.g., in the exponential tail of the Fourier transform of the velocity field. In lower dimensions, such as the one-dimensional Burgers equation with the usual (Laplacian) dissipation, the problem of finite-time blow-up and its relation to complex singularities is completely understood [16].

Although the Navier-Stokes equation, with  $\nu \rightarrow 0$  and suitable initial conditions, provides a complete description of the velocity field  $\mathbf{u}$  in space and time, the pitfalls of a theoretical treatment of such an equation, at small scales in particular, is best illustrated by the following: At small scales, the properties of the solutions of the Navier-Stokes equation can be conveniently studied by neglecting the nonlinear convection term yielding  $\hat{u}_k \sim e^{-(k/k_d)^2}$ , where  $k_d$  is the energy dissipation wavenumber. However, more refined theoretical arguments, based on the analytic properties of velocity fields at small scales [17] or on some estimates of velocity field correlations [18] suggest an exponential decay as  $k \rightarrow \infty$ . Indeed, direct numerical simulations suggest that the energy spectrum, at large  $k$ , is consistent with the functional form  $(k/k_d)^\gamma e^{-\delta(k/k_d)}$  [19, 20]. The constant  $\delta$  is believed to be a Reynolds number dependent quantity, whereas  $\gamma$  is expected to be universal. The exact numerical value of  $\gamma$  is unknown and the only prediction so far is based on Kraichnan's DIA equations [21] giving  $\gamma = 3$ .

The large- $k$  asymptotic discussed above is relevant, of course, to the deep dissipation range and have their roots in issues of regularity and finite-time blow-up of solutions of the incompressible Navier-Stokes and Euler equations. For moderate values of  $k$ , in the so-called inertial range where the ideas of Kolmogorov hold, the energy spectrum  $E(k) \sim k^{-5/3}$  (up to intermittency corrections). Between this intermediate and the large- $k$  asymptotics, lies the bottleneck region. The bottleneck is defined as a bump in the turbulence spectrum which leads to a non-monotonic behaviour in a narrow range of scales between the inertial and dissipation range (an instance of a bottleneck in a numerical simulation can be found in [22]). It has been argued that this pile-up is due to suppression of energy transfer to smaller scales by the

action of dissipation [23]. However, to the best of our knowledge analytical predictions of the flow at bottleneck scales have not been checked against numerical or experimental data so far, particularly because the pile-up effect is only weakly pronounced at the currently available Reynolds numbers.

We propose a novel approach to understand the dissipation and the transitional (bottleneck) ranges through modifying the standard Laplacian dissipation term  $\nu\Delta\mathbf{u}$  by a more general function  $f(\sqrt{-\Delta})$  (or in the Fourier space  $f(|\mathbf{k}|)$ ). An instance of such a dissipation term is the well-known hyperviscous dissipation term  $\nu(-\Delta)^\alpha$  which is frequently used in numerical simulations. Clearly, the constants  $\gamma$  and  $\delta$  determining the behavior of the energy spectrum in the dissipation range change with  $\alpha$ , in particular the fall-off of the spectrum becomes steeper with growing  $\alpha$ . The bottleneck has been shown to become more pronounced with increasing  $\alpha$ , see, e.g., Ref. [24, 25, 26, 27] as well as Ref. [28] for a review, allowing for theoretical calculations, in the large  $\alpha$  limit to be checked against numerical simulations. It is also important to remember that the use of hyperviscosity has shed light on the problem of finite-time blow-up: It was shown [12, 29] that there is no finite-time blow-up for  $\alpha > 5/4$  despite the existence of complex singularities. For more general dissipative functions, there is one example that we know of where the dissipative term of the form  $f(|\mathbf{k}|) = \exp(|\mathbf{k}|)$  leads to entire solutions [30].

In this paper, by using a generalised dissipative term  $f(\sqrt{-\Delta})$ , we revisit the problem of the nature of the velocity field in the far dissipation range as well as derive analytical results in the bottleneck region which connects the intermediate asymptotics of the inertial range to the true asymptotics of the far dissipation range. However, the use of such a generalised dissipation is not completely amenable to a rigorous theoretical treatment. This is because, as is well-known, since Euler's discovery of the equations for ideal fluids more than 250 years ago, we are still far from having a complete analytical handle of the nature of the velocity field in viscous and idealised fluids. We therefore resort to a simpler model, namely that of the one-dimensional Burgers equation [31], which, while retaining the same structure of the non-linearity in the Euler and Navier-Stokes equations, allow for a more rigorous analytical treatment [16, 32, 33]. Most of our results are easily generalisable to higher dimensional equations of hydrodynamics; we shall comment on these later.

Our paper is organised as follows. We begin our investigations in Section 2 by considering solutions of the one-dimensional (compressible) Burgers equation with modified dissipation

$$\partial_t u + u\partial_x u = -f(\sqrt{-\partial_x^2}) u. \quad (1)$$

The approach that we use can be easily generalized to other hydrodynamical equations such as the Navier–Stokes equations. We show that the leading order contribution to such solutions can be calculated recursively from an algebraic recursion relation involving iterated integrations. Furthermore, in the limit of large times this recursion relation can be transformed to a simple algebraic recursion relation. All of these considerations apply not only to hydrodynamical equation with the standard viscous term but also allow for more general viscous terms such as hyperviscous or exponentially growing dissipation terms [30].

In Section 3 we investigate the transition region between the dissipation range and the inertial range. In the case of the Burgers equation, the bottleneck in the spectrum is present only in the hyperviscous case when  $\alpha > 1$ . Motivated by the recent work of Frisch, *et al.*, [26] we investigate how the presence of the bottleneck is related to Gibbs-type oscillations in the velocity field arising in the neighbourhood of strongly dissipating structures. In the framework of the one-dimensional Burgers equation the method of matched asymptotics can be used to derive a simplified equation for such structures which in this case are shocks [34]. It is known that one can determine the asymptotics of the (oscillatory) solutions of this simplified equation. However, since neither the amplitude nor the phase of these oscillations is known, we determine them numerically and show that the asymptotic solution indeed gives the right description of the bottleneck. We also derive analytical relations which allow us to estimate for what kind of dissipation term the simplified boundary layer Burgers equation will exhibit a bottleneck.

In Section 4 we compare the analytical and semi-analytical results of Sections 2 and 3 with state-of-the-art direct numerical simulations. By using high-precision simulations and asymptotic extrapolation of sequences [36] we determine the asymptotic structure of solutions in the dissipation range and compare it with theoretical results. We also show that asymptotic solutions of the boundary layer Burgers equation obtained in Section 3 are in agreement with the numerical solutions in the bottleneck region.

In the last section, we discuss the implications of the results proved in the earlier sections and make concluding remarks.

## **2. Solutions of the Burgers equation with modified dissipation**

The solution of the  $d$ -dimensional Burgers equation with standard (Laplacian) dissipation, in the limit of vanishing viscosity, has been studied extensively, and successfully, by using various techniques [16, 34]. However, these established analytical approaches are limited in scope when applied to the present problem of the Burgers equation with a dissipation term which is not necessarily a Laplacian. This is because in the dissipation range, such methods rarely allow us to determine beyond the leading order asymptotics. A second drawback – which holds even for the usual Laplacian dissipation – is the reliance of conventional techniques on properties peculiar to the Burgers equation. Consequently, generalising for the higher dimensional Euler and Navier-Stokes equations have proved formidable.

Given this, we present an approach which does not rely on the specific properties of the one-dimensional Burgers equation and hence can be generalized to the multi-dimensional Navier–Stokes equation. This approach is in the spirit of recent studies by Lee and Sinai of several hydrodynamic equations with complex-valued initial conditions as well as for the case of a bounded domain with periodic boundary conditions. Of course, we should note, that if one were to be interested only in the one-dimensional Burgers equation, other theoretical methods are more efficient; the advantage of our approach lies in it being easily adapted to multidimensional equations of hydrodynamics.

We will consider two cases: (i) initial conditions which are real-valued in the physical

space but have compact support in the Fourier space and (ii) initial conditions whose initial Fourier modes are supported on the positive half-axis (such initial conditions are necessarily complex-valued in the physical space).

### 2.1. Real-Valued Initial Conditions

By using the semi-group  $e^{-tf(\sqrt{-\partial_x^2})}$ , generated by  $-f(\sqrt{-\partial_x^2})$ , and the Duhamel principle [35], Eq. (1) can be written as

$$u(x, t) = - \int_0^t e^{-(t-s)f(\sqrt{-\partial_x^2})} u(x, s) \partial_x u(x, s) ds, \quad (2)$$

or in the Fourier space representation

$$\hat{u}(k, t) = \hat{u}(k, 0) e^{-f(k)t} - \frac{ik}{2} \sum_{l+l'=k} e^{-f(k)t} \int_0^t e^{f(k)s} \hat{u}(l, s) \hat{u}(l', s) ds. \quad (3)$$

Here, and in the following, we assume that the generalised dissipation function  $f(k)$  is a positive, non-decreasing, strictly convex even function of  $k$  with  $f(0) = 0$ .

We now introduce an explicit dependence on the amplitude of the initial condition via

$$u(x, t)|_{t=0} = Au_0(x). \quad (4)$$

Here, when all other parameters are fixed,  $A$  plays the role of the Reynolds number. We now expand the solution corresponding to the initial condition (4) in a formal power series in  $A$

$$u(x, t) = \sum_{n=1}^{\infty} u^{(n)}(x, t) A^n; \quad (5)$$

for suitable initial conditions, this series has a non-vanishing radius of convergence [37].

Furthermore,  $u^{(n)}$  satisfy the recurrence relations

$$u^{(1)} = \exp \left[ -tf(\sqrt{-\partial_x^2}) \right] u_0, \quad (6)$$

for  $n = 1$  and

$$u^{(n)} = - \int_0^t \exp \left[ -(t-s)f(\sqrt{-\partial_x^2}) \right] \sum_{m=1}^{n-1} u^{(m)}(s) \partial_x u^{(n-m)}(s) ds, \quad (7)$$

for  $n > 1$ . In the Fourier space representation we use, for convenience,  $\hat{u}(k, t) = i\hat{v}(k, t)$ , so that the respective recursion relations become

$$\hat{v}^{(1)}(k, t) = \hat{v}_0(k) e^{-f(k)t} \quad (8)$$

and

$$\hat{v}^{(n)}(k, t) = \frac{k}{2} \sum_{l+l'=k} e^{-f(k)t} \int_0^t e^{f(k)s} \sum_{m=1}^{n-1} \hat{v}^{(m)}(l, s) \hat{v}^{(n-m)}(l', s) ds. \quad (9)$$

By using these recursive formulas it is easy to make the following observation:

**Prop. 2.1** *Suppose that  $\hat{v}_0(k)$  is supported only by finitely many modes in the Fourier space, i.e.,  $k \in \Sigma = \{-K, \dots, K\}$ , where  $K$  is a positive integer. Then for any  $n \geq 2$  the function  $\hat{v}^{(n)}(k, t)$  also has a finite support in the Fourier space  $n\Sigma = \{-nK, \dots, nK\}$  and every  $\hat{v}^{(n)}(k, t)$  can be calculated by finitely many operations.*

This observation can be used to calculate recursively solutions of Eq.( 1) in a manner similar to the recursive calculation of solutions of inviscid equations by means of time series expansions. Here we demonstrate this on the example of initial conditions consisting of one Fourier mode  $u_0(x) = \sin x$ . Then the first two terms of the expansion are

$$u^{(1)}(x, t) = \sin x e^{-tf(1)}, \quad (10)$$

and

$$u^{(2)}(x, t) = -\frac{1}{2} \frac{1}{f(2) - 2f(1)} \sin 2x \left( e^{-2f(1)t} - e^{-f(2)t} \right). \quad (11)$$

It is not difficult to verify that the higher order terms are of the form

$$u^{(n)}(x, t) = g_0^{(n)}(t) \sin nx + g_2^{(n)}(t) \sin(n-2)x + \dots \quad (12)$$

This representation can be easily transferred into the Fourier representation as

$$v^{(n)}(n, t) = -\frac{1}{2} g_0^{(n)}(t), \quad v^{(n)}(n-2, t) = -\frac{1}{2} g_2^{(n)}(t), \quad \dots \quad (13)$$

$$v^{(n)}(-n, t) = \frac{1}{2} g_0^{(n)}(t), \quad v^{(n)}(-n+2, t) = \frac{1}{2} g_2^{(n)}(t), \quad \dots \quad (14)$$

We now note that although for a fixed wavenumber  $k$  obtaining  $\hat{v}(k, t)$  requires summation of the whole series in  $A$ , to obtain small- $A$  asymptotics it suffices to consider only the lowest power of  $A$  for a given  $k$ . For the initial condition  $\sin x$  this lowest power for wavenumber  $k$  is  $A^k$  and we obtain the following small  $A$  asymptotics

$$\hat{v}(k, t) \sim \hat{v}_{\text{as}}(k, t) = A^{-k} \hat{v}^{(-k)}(k, t) \quad k < 0; \quad (15)$$

$$\hat{v}(k, t) \sim \hat{v}_{\text{as}}(k, t) = A^k \hat{v}^{(k)}(k, t) \quad k > 0. \quad (16)$$

The function  $\hat{v}_{\text{as}}(k, t)$  can be represented as a sum of two functions  $\hat{v}_{\text{as}}^+(k, t)$  and  $\hat{v}_{\text{as}}^-(k, t)$  with support on the positive and negative half-axis, respectively. The function  $\hat{v}_{\text{as}}^+(k, t)$  is the solution of the recurrent equation (for  $k > 0$ )

$$\hat{v}_{\text{as}}^+(k, t) = \hat{v}(k, 0) e^{-f(k)t} + \frac{k}{2} \sum_{l=1}^{k-1} e^{-f(k)t} \int_0^t e^{f(k)s} \hat{v}_{\text{as}}^+(l, s) \hat{v}_{\text{as}}^+(k-l, s) ds. \quad (17)$$

The function  $\hat{v}_{\text{as}}^-(k, t)$  satisfies an analogous equation with  $k < 0$ . Let us stress that the functions  $\hat{v}_{\text{as}}^+(k, t)$  and  $\hat{v}_{\text{as}}^-(k, t)$  are also solutions of the Burgers equation, however, with one-mode *complex-valued* initial conditions. The function  $\hat{v}_{\text{as}}^+(k, t)$  corresponds to the initial condition  $\hat{v}_{\text{as}}^+(1, 0) = A\hat{v}_0(1)$  and the function  $\hat{v}_{\text{as}}^-(k, t)$  to the initial conditions  $\hat{v}_{\text{as}}^-(-1, 0) = A\hat{v}_0(-1)$ . The asymptotic solution in the physical space  $u_{\text{as}}(x, t)$  can be written in terms of the coefficients  $g_0^{(n)}(t)$

$$u_{\text{as}}(x, t) = \sum_{n=1}^{\infty} g_0^{(n)}(t) \sin nx A^n, \quad (18)$$

where

$$g_0^{(n)}(t) = \sum_{\alpha_1 + 2\alpha_2 + \dots + n\alpha_n = n} \frac{1}{2^{n-1}} G(n; \alpha_1, \alpha_2, \dots, \alpha_n) e^{-t(\alpha_1 f(1) + \alpha_2 f(2) + \dots + \alpha_n f(n))}. \quad (19)$$

The sum is taken over all combinations of  $n$  non-negative integers  $\alpha_i$ ,  $i = 1, \dots, n$  such that  $\alpha_1 + 2\alpha_2 + \dots + n\alpha_n = n$ . We note that these combinations correspond to partitions of integers. For example, for  $n$  from 1 to 4, we obtain the following combinations:

- $n = 1$ :  $\{(\alpha_1)\} = \{(1)\}$ ,
- $n = 2$ :  $\{(\alpha_1, \alpha_2)\} = \{(2, 0), (0, 1)\}$ ,
- $n = 3$ :  $\{(\alpha_1, \alpha_2, \alpha_3)\} = \{(3, 0, 0), (1, 1, 0), (0, 0, 1)\}$ ,
- $n = 4$ :  $\{(\alpha_1, \alpha_2, \alpha_3, \alpha_4)\} = \{(4, 0, 0, 0), (2, 1, 0, 0), (0, 2, 0, 0), (1, 0, 1, 0), (0, 0, 0, 1)\}$ .

The recurrence relation for coefficients  $G(n; (n, 0, \dots, 0))$ ,  $n \geq 1$  corresponding to combinations  $(n, 0, \dots, 0)$  is

$$G(n; (n, 0, \dots, 0)) = -\frac{n}{2} \frac{1}{f(n) - nf(1)} \sum_{m=1}^{n-1} G(m; (m, 0, \dots, 0)) G(n-m; (n-m, 0, \dots, 0)).$$

Note that these coefficients contribute to terms with decay rate  $e^{-ntf(1)}$ , which is the slowest decay rate possible for  $g_0^{(n)}(t)$ . For coefficients  $G(n; (n-2, 1, 0, \dots, 0))$ ,  $n \geq 3$  of combinations  $(n-2, 1, 0, \dots, 0)$ , we obtain

$$\begin{aligned} G(n; (n-2, 1, 0, \dots, 0)) &= -\frac{n}{f(n) - (n-2)f(1) - f(2)} G(n-1, (n-3, 1, 0, \dots, 0)) - \\ &\frac{n}{2} \frac{1}{f(n) - (n-2)f(1) - f(2)} \sum_{m=2}^{n-2} \left[ G(m; (m, 0, \dots, 0)) G(n-m; (n-m-2, 1, 0, \dots, 0)) + \right. \\ &\left. G(m; (m-2, 1, 0, \dots, 0)) G(n-m; (n-m, 0, \dots, 0)) \right]. \end{aligned} \quad (20)$$

Generally, for coefficients  $G(n; (\alpha_1, \dots, \alpha_{n-1}, 0))$  of combinations of the type  $(\alpha_1, \dots, \alpha_{n-1}, 0)$ , where the last entry vanishes, we obtain the relation

$$\begin{aligned} G(n; (\alpha_1, \dots, \alpha_{n-1}, 0)) &= -\frac{n}{2} \frac{1}{f(n) - \alpha_1 f(1) - \dots - \alpha_{n-1} f(n-1)} \\ &\sum_{m=1}^{n-1} \sum_{\underline{\beta} + \underline{\gamma} = \underline{\alpha}} G(m; (\beta_1, \dots, \beta_m)) G(n-m; (\gamma_1, \dots, \gamma_{n-m})). \end{aligned} \quad (21)$$

Here we denote  $\underline{\alpha} = (\alpha_1, \dots, \alpha_{n-1}) \in \mathbb{N}_0^{n-1}$ ,  $\underline{\beta} = (\beta_1, \dots, \beta_m, 0, \dots, 0) \in \mathbb{N}_0^{n-1}$  and  $\underline{\gamma} = (\gamma_1, \dots, \gamma_{n-m}, 0, \dots, 0) \in \mathbb{N}_0^{n-1}$ , where  $\beta_1 + 2\beta_2 + \dots + m\beta_m = m$  and  $\gamma_1 + 2\gamma_2 + \dots + (n-m)\gamma_{n-m} = n-m$ . Coefficients  $G(n; (0, 0, \dots, 0, 1))$  can be calculated from the coefficients corresponding to combinations with  $\alpha_n = 0$

$$\begin{aligned} G(n; (0, 0, \dots, 0, 1)) &= \sum_{m=1}^{n-1} (n-m) \sum_{\alpha_1 + 2\alpha_2 + \dots + m\alpha_m = m} \sum_{\beta_1 + 2\beta_2 + \dots + (n-m)\beta_{n-m} = n-m} \\ &\frac{G(m; \alpha_1, \alpha_2, \dots, \alpha_m) G(n-m; \beta_1, \beta_2, \dots, \beta_{n-m})}{f(n) - \alpha_1 f(1) - \alpha_2 f(2) - \dots - \alpha_m f(m) - \beta_1 f(1) - \beta_2 f(2) - \dots - \beta_{n-m} f(n-m)}. \end{aligned} \quad (22)$$

We note that in the case, when the function  $f(\cdot)$  describe the standard dissipation  $-\nu \partial_x^2$  the coefficients  $G(\cdot; \cdot)$  can be found explicitly by means of the Hopf-Cole transformation which yields the familiar expression

$$u(x, t) = -2\nu \ln \left( e^{t\nu \partial_x^2} e^{-\frac{A}{2\nu} u_0} \right). \quad (23)$$

## 2.2. Solutions of the one-dimensional Burgers equation for complex-valued initial conditions

As has been noted in Ref. [30], for initial conditions supported on the positive half-line, i.e.,  $\hat{v}(k, 0) = 0$  for  $k \leq 0$ , the Fourier coefficient of the solution at a fixed wavenumber can be calculated iteratively by finitely many operations via Eq. (17). Thus, e.g., we obtain

$$\hat{v}(1, t) = \hat{v}_0(1) e^{-f(1)t}, \quad (24)$$

$$\hat{v}(2, t) = \left[ \hat{v}_0(2) - \frac{1}{f(2) - 2f(1)} \hat{v}_0^2(1) \right] e^{-f(2)t} + \frac{\hat{v}_0^2(1) e^{-2f(1)t}}{f(2) - 2f(1)} \quad (25)$$

and

$$\begin{aligned} \hat{v}(3, t) &= \left\{ \hat{v}_0(3) - \frac{3\hat{v}_0(1)\hat{v}_0(2)}{f(3) - f(1) - f(2)} \right. \\ &+ \frac{3\hat{v}_0^3(1)}{f(2) - 2f(1)} \left[ \frac{1}{f(3) - f(1) - f(2)} - \frac{1}{f(3) - 3f(1)} \right] \left. \right\} e^{-f(3)t} \\ &+ 3 \left[ \hat{v}_0(1)\hat{v}_0(2) - \frac{\hat{v}_0^3(1)}{f(2) - 2f(1)} \right] \frac{e^{-[f(1)+f(2)]t}}{f(3) - f(1) - f(2)} \\ &+ \frac{3\hat{v}_0^3(1)e^{-3f(1)t}}{[f(2) - 2f(1)][f(3) - 3f(1)]}. \end{aligned} \quad (26)$$

In general the Fourier coefficients of the solution will have a form which is similar to Eq. (19)

$$\hat{v}(k, t) = \sum_{\alpha_1+2\alpha_2+\dots+k\alpha_k=k} F(k; (\alpha_1, \alpha_2, \dots, \alpha_k)) e^{-t(\alpha_1 f(1) + \alpha_2 f(2) + \dots + \alpha_k f(k))}. \quad (27)$$

It is instructive to compare this form with the explicit expression found in the case of  $f(\sqrt{-\partial_x^2}) = -\nu \partial_x^2$  and  $u_0(x) = Ae^{ix}$  obtained by using Faà di Bruno's formula

$$\begin{aligned} \hat{u}(k, t) &= -2\nu \frac{(-1)^k A^k}{k!} \frac{1}{2^k \nu^k} \sum_{l=1}^k (-1)^{l-1} (l-1)! \sum_{j_1, j_2, \dots, j_{k-l+1}} \frac{k!}{j_1! j_2! \dots j_{k-l+1}!} \times \\ &\left( \frac{1}{1!} \right)^{j_1} \left( \frac{1}{2!} \right)^{j_2} \dots \left( \frac{1}{(k-l+1)!} \right)^{j_{k-l+1}} e^{-\nu t(j_1 + j_2 2^2 + \dots + j_{k-l+1} (k-l+1)^2)}, \end{aligned} \quad (28)$$

where the second sum is taken over  $k-l+1$  nonnegative integers  $j_1, \dots, j_{k-l+1}$  such that

$$j_1 + j_2 + \dots + j_{k-l+1} = l,$$

and

$$j_1 + 2j_2 + \dots + (k-l+1)j_{k-l+1} = k.$$

In the explicit solution, the dependence on the amplitude of the initial condition  $A$  manifests itself by the term  $A^k$ , in agreement with the observation made previously. The time dependence is also clearly exhibited by the terms  $e^{-\nu t(j_1 + j_2 2^2 + \dots + j_{k-l+1} (k-l+1)^2)}$ , which in the more general case become  $e^{-t(\alpha_1 f(1) + \alpha_2 f(2) + \dots + \alpha_k f(k))}$ . Finally, the exact solution also gives explicit expressions for the coefficients  $F(k; (\alpha_1, \alpha_2, \dots, \alpha_k))$ .

In general, calculating solutions of the Burgers equation with modified dissipation by recursive determination of coefficients  $F(k; (\alpha_1, \alpha_2, \dots, \alpha_k))$  is quite cumbersome. We now take advantage of the fact that in the limit of large times the terms with exponential decay  $e^{-kf(1)}$  dominate over the other terms.



**Prop. 2.2** From the assumptions on  $f(\cdot)$ , it follows that  $f(\cdot)$  is a super-additive function. The term in the sum on the right-hand-side of Eq. (27) with the slowest decay in  $t$  corresponds to  $(\alpha_1, \alpha_2, \dots, \alpha_k) = (k, 0, \dots, 0)$ , with the rate of temporal decay  $e^{-kf(1)t}$ . The coefficient  $F(k, (k, 0, \dots, 0)) = h(k)$  satisfies the following recursion relation

$$h(k) = \frac{k}{2} \frac{1}{f(k) - kf(1)} \sum_{l=1}^{k-1} h(l) h(k-l), \quad (29)$$

with  $h(1) = \hat{v}_0(1)$ . Thus, for a fixed  $k$  and  $t \rightarrow +\infty$

$$\hat{v}(k, t) \sim F(k, (k, 0, \dots, 0)) e^{-kf(1)t}. \quad (30)$$

Note that the high wavenumber contributions to the initial conditions are suppressed when  $t \rightarrow \infty$  and the solution therefore becomes independent of the initial condition since the  $k$ th mode is proportional to  $\hat{v}_0^k(1)$ . Thus, the behaviour of solutions of Eq. (3) is universal at large times.

### 2.3. Reduction to an ordinary difference-differential equation

To study the solutions of the recursion relation Eq. (29), we introduce the generating function  $h(x)$  of  $h(k)$

$$h(x) = \sum_{k=1}^{\infty} h(k) e^{kx}, \quad (31)$$

so that Eq. (29) becomes an ordinary pseudo-differential equation

$$f(\partial_x) h - f(1) \partial_x h = \frac{1}{2} \partial_x h^2, \quad (32)$$

with boundary conditions  $h(x) \sim \hat{v}_0(1)e^x$  for  $x \rightarrow -\infty$ . It is well-known that the asymptotic properties of  $h(k)$  can be deduced from the analytic properties of  $h(\xi)$ . Here we will consider two cases: (i) hyperviscosity

$$f_1(k) = k^{2\alpha}, \quad (33)$$

and (ii) exponentially growing dissipation

$$f_2(k) = e^k. \quad (34)$$

In case (i) the solution  $h(x)$  has a singularity at some point  $x_0$ . We know that the solution of Eq. (32) in the neighborhood of the singularity behaves as  $(x - x_0)^{2\alpha-1}$

$$h(x) = \frac{1}{(x - x_0)^{2\alpha-1}} g(x - x_0). \quad (35)$$

To determine higher-order contributions, we assume that the function  $g(x - x_0)$  can be written as

$$g(x - x_0) = g^{(1)}(x - x_0) + (x - x_0)^\gamma g^{(2)}(x - x_0) + \text{h.o.t.}, \quad (36)$$

where the functions  $g^{(1)}(x - x_0)$  and  $g^{(2)}(x - x_0)$  are analytic with Taylor expansions

$$g^{(1)}(\xi) = \sum_{l=0}^{\infty} g_l^{(1)} \xi^l, \quad g^{(2)}(\xi) = \sum_{l=0}^{\infty} g_l^{(2)} \xi^l; \quad (37)$$

and the remaining terms are of higher, non-integer orders. Inserting the representations (35) and (36) into Eq. (32), we obtain the following equation for  $\gamma$

$$\sum_{m=0}^{2\alpha-2} (-1)^m \binom{2\alpha-1}{m} \frac{(2\alpha-2+m)!}{(2\alpha-2)!} (\gamma)_{2\alpha-1-m} + \frac{(4\alpha-3)!}{(2\alpha-2)!} = 0. \quad (38)$$

Here  $(\gamma)_{2\alpha-m-1}$  is the Pochhammer symbol. One solution is  $\gamma = -1$ ; the other solutions are complex and we denote them by  $\gamma_i^\pm$ ,  $i = 1, \dots, \alpha-1$ , with  $Re(\gamma_i^\pm) > 0$  and  $(\gamma_i^+)^* = \gamma_i^-$ . The terms  $(x-x_0)^{\gamma_i^\pm}$  imply that the asymptotic expansion of  $h(k)$  for  $k \rightarrow \infty$  has the form

$$h(k) \simeq C k^{2\alpha-2} e^{-\delta k} \left( 1 + \frac{b_1}{k} + \dots + \sum_{i=1}^{\alpha-1} c_1^i k^{-\gamma_i^+} + \sum_{i=1}^{\alpha-1} (c_1^i)^* k^{-\gamma_i^-} + \dots \right) \quad (39)$$

For case (ii), Eq. (32) becomes a difference-differential equation

$$h(x+1) = \partial_x \left\{ \frac{1}{2} h^2(x) + e^1 h(x) \right\}. \quad (40)$$

Solutions of this equation are entire functions [30]; therefore we concentrate on their behaviour for  $x \rightarrow \infty$ . Assuming that  $h(x) \rightarrow \infty$  for  $x \rightarrow \infty$  we write  $h(x) = \exp[S(x)]$  obtaining

$$e^{S(x+1)} = \partial_x \left\{ e^{2S(x)} + e^{S(x)+1} \right\}. \quad (41)$$

The dominant behaviour can be deduced from the relation

$$S(x+1) = 2S(x), \quad (42)$$

which is solved by

$$S(x) = \beta(x) e^{x \ln 2}. \quad (43)$$

Here  $\beta(x)$  is a periodic function with period 1:  $\beta(x+1) = \beta(x)$ . Thus, to the leading order the solution is given by

$$H(x) = \exp [\beta(x) e^{x \ln 2}]. \quad (44)$$

From this representation it is easy to determine the behaviour of  $h(k)$  as follows: Introducing a new variable  $\xi = e^x$  we see that  $h(k)$  are the Taylor coefficients of  $\tilde{h}(\xi) = h(\ln e^x)$  and that for  $\xi \rightarrow \infty$

$$\tilde{h}(\xi) \sim \exp [\beta(\ln \xi) \xi^{\ln 2}]. \quad (45)$$

The function  $\tilde{h}(\xi)$  is thus an entire function of order  $\ln 2$ . It is well-known that the growth rate of entire functions at infinity determines the behavior of their Taylor coefficients for  $k \rightarrow \infty$  [39] so that

$$h(k) \sim e^{-\frac{1}{\ln 2} k \ln k}. \quad (46)$$

Actually, the asymptotic behaviour of  $h(k)$  can be determined directly from the recursion relation for  $h(k)$  along with sub-dominant terms

$$h(k) \simeq \frac{1}{2^{\frac{3}{2}} \sqrt{\pi \ln 2}} k^{-\frac{3}{2}} e^{(\delta+g(\ln k))k} e^{-\frac{1}{\ln 2} k \ln k}, \quad (47)$$

where the function  $g(\cdot)$  is periodic with period  $\ln 2$ . The presence of the function  $g(\ln k)$  in the asymptotic expansion of  $h(k)$  is related to the presence of the function  $\beta(x)$  in the expansion of  $h(x)$  at infinity.

Finally, we remark that the estimate (46) of the dominant part in the high wavenumber asymptotics of solutions of the Burgers equation with exponentially growing dissipation can be proved rigorously [37].

### 3. Bottleneck effect in the boundary layer of the one-dimensional Burgers equation

The analysis presented in the previous section applies only to small Reynolds numbers and can thus be relevant only for the dissipation range. To study the transition zone between the dissipation range and the inertial range we have to take recourse to asymptotic matching which so far is known to work only for the Burgers equation. We write the Burgers equation with modified dissipation in the form

$$\partial_t u + u \partial_x u = -\frac{1}{\nu} f(\nu \sqrt{-\partial_x^2}) u. \quad (48)$$

In the limit of vanishing viscosity  $\nu \rightarrow 0$  the *outer* solution, which is the entropic solution of the inviscid Burgers equation, is matched against the *inner* solution of the equation

$$f\left(\sqrt{-\frac{d^2}{dX^2}}\right) u^{(\text{in})} + u^{(\text{in})} \frac{d}{dX} u^{(\text{in})} = 0, \quad (49)$$

satisfying the boundary conditions  $\lim_{X \rightarrow -\infty} u^{(\text{in})}(X) = 1$  and  $\lim_{X \rightarrow +\infty} u^{(\text{in})}(X) = -1$  [26, 40]. In this section we shall study various aspects of solutions of the inner equation (49), in particular, with an eye on the bottleneck effect.

#### 3.1. Bottleneck and oscillations

Equation (49), for the case of the hyperviscous dissipation term  $f(k) = k^{2\alpha}$ , has been studied by asymptotic and numerical methods in Refs. [26, 34]. The same methods are easily extended to Eq. (49) for more general dissipation terms. Thus, in the case of a more general  $f(k)$  (here, we only assume that it grows faster than linearly) we can use asymptotic expansion of the solution at  $\pm\infty$ : neglecting nonlinear contributions Eq. (49) is written as

$$f\left(\sqrt{-\frac{d^2}{dX^2}}\right) u_{\text{as}}^{(\text{in})} + \frac{d}{dX} u_{\text{as}}^{(\text{in})} = 0, \quad X \rightarrow -\infty, \quad (50)$$

$$f\left(\sqrt{-\frac{d^2}{dX^2}}\right) u_{\text{as}}^{(\text{in})} - \frac{d}{dX} u_{\text{as}}^{(\text{in})} = 0, \quad X \rightarrow +\infty. \quad (51)$$

By using the *ansatz*  $u_{\text{as}}^{(\text{in})} = e^{-i\zeta x}$  and  $u_{\text{as}}^{(\text{in})} = e^{i\zeta x}$  we obtain an equation for  $\zeta$

$$\frac{1}{\zeta} f(\zeta) = i. \quad (52)$$

The boundary conditions imply that we take only those solutions  $\zeta_i$  of Eq. (52) for which  $\text{Im } \zeta_i > 0$ . Let us consider the solution  $\zeta_{\min}$  of Eq. (52) with the smallest imaginary part  $\text{Im } \zeta_{\min}$ . The leading order asymptotics for  $X \rightarrow \pm\infty$  are

$$\begin{aligned} u^{(\text{in})}(X) &\simeq u_{\text{as}}^{(\text{in})}(X) = 1 - Ae^{\lambda X} \sin(\omega X + \phi), & X \rightarrow -\infty; \\ u^{(\text{in})}(X) &\simeq u_{\text{as}}^{(\text{in})}(X) = -1 - Ae^{-\lambda X} \sin(\omega X - \phi), & X \rightarrow +\infty; \end{aligned} \quad (53)$$

where  $\lambda = \text{Im } \zeta$  and  $\omega = \text{Re } \zeta$  and  $A$  is chosen to be positive. In the case when  $\text{Re } \lambda_{\min} \neq 0$ , the solution oscillates around  $\pm 1$ . However, neither the amplitude of the oscillation  $A$ , nor the phase  $\phi$  can be determined from a linear analysis.

The Fourier transform of the linearized solution is

$$\hat{u}_{\text{as}}^{(\text{in})}(k) = -i\sqrt{\frac{2}{\pi}} \frac{1}{k} - i\sqrt{\frac{2}{\pi}} A k \frac{k^2 \sin \phi + \lambda^2 \sin \phi - 2\lambda\omega \cos \phi - \omega^2 \sin \phi}{(\lambda^2 + \omega^2 - 2\omega k + k^2)(\lambda^2 + \omega^2 + 2\omega k + k^2)}. \quad (54)$$

At high  $k$  the linearized asymptotic solution  $\hat{u}_{\text{as}}^{(\text{in})}(k)$  decays as  $-i\sqrt{2/\pi}(1 + A \sin \phi)k^{-1}$  contrary to the actual solutions of Eq. (49) which decay exponentially or faster than exponentially. Nevertheless, we expect that the dissipation range is being mimicked also for the linearized asymptotic solution: For high  $k$  the asymptotic solution has to decrease faster than the small  $k$  solution  $-i\sqrt{2/\pi}k^{-1}$  and this is possible only when  $A \sin \phi < 0$  as confirmed by numerical simulations.

In Fig. (1), we compare numerical solutions and linearized asymptotic solutions for the hyperviscous dissipation term  $f(k) = k^{2\alpha}$  with  $\alpha = 4, 5, 6$ . The agreement between the two is

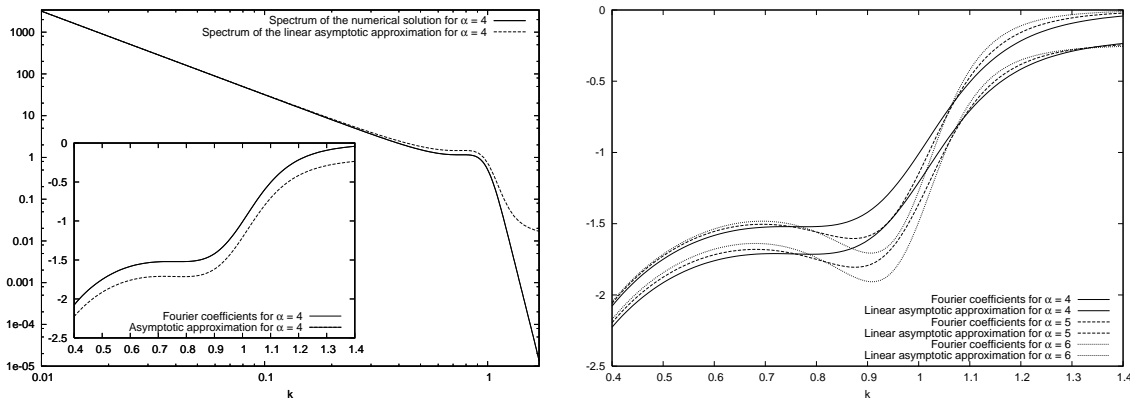


**Figure 1.** Comparison between the imaginary part of numerical solution of Eq. (49) in the Fourier space and the imaginary part of the linearized asymptotic solution Eq. (53) in the Fourier space for  $f(k) = k^8$  (solid lines),  $f(k) = k^{10}$  (dashed lines) and  $f(k) = k^{12}$  (dotted lines). Note that in the bottleneck region the numerical and the asymptotic solutions have the same shape with the asymptotic solution shifted down compared to the numerical solution.

remarkably good, in particular in the bottleneck region they seem to have similar shapes. We do note, however, that the linear asymptotic solution is shifted with respect to the complete solution. Thus, although the expression (54) is an excellent model for the solution in the bottleneck region, there is a drawback: The amplitude  $A$  and the phase shift  $\phi$  cannot be determined analytically and has to be extracted numerically.

Now we derive an integral identity for solutions of Eq. (49). We multiply Eq. (49) by  $G(u^{(\text{in})})$  and integrate over  $X$ , obtaining

$$\int_{\mathbb{R}} G(u^{(\text{in})}) f \left( \sqrt{-\frac{d^2}{dX^2}} \right) u^{(\text{in})} dX = g(1) - g(-1), \quad (55)$$

where the functions  $G(\cdot)$  and  $g(\cdot)$  are related by

$$\frac{d}{du} g(u) = uG(u). \quad (56)$$

For  $G(u) = u$ , we obtain the relation

$$\int_{\mathbb{R}} f(k) |\hat{u}^{(\text{in})}(k)|^2 dk = \frac{2}{3}. \quad (57)$$

We divide the Fourier space into three ranges: the small wave-number range  $(-k_i, k_i)$ , corresponding to the inertial range, the intermediate wave-number range  $(-k_d, -k_i) \cup (k_i, k_d)$  and the high wave-number range  $(-\infty, -k_d) \cup (k_d, +\infty)$  which corresponds to the dissipation range. Because of the exponential decay of the Fourier coefficients in the dissipation range the contribution to the integral (57) from the high wave-number range is negligible.

To a first approximation, we estimate the width of the small wave-number range  $(-k_i, k_i)$  by assuming that the entire contribution to (57) comes from this range

$$\frac{2}{\pi} \int_{-k_i}^{k_i} \frac{f(k)}{k^2} dk = \frac{2}{3}. \quad (58)$$

Obviously, the solution of Eq. (58) gives an upper bound for the higher end of the inertial range. By setting  $f(k_d) = 1$  at the lower end of the dissipation range, we estimate the beginning of the dissipation range. For the definitions of  $k_i$  and  $k_d$  to be consistent we require that  $k_i < k_d$ . However, for  $f(k)$  such that  $f(k)/k^2$  are small for small  $k$  this consistency condition is violated.

Consider for example a dissipation term given by  $f(k) = k^4 + ak^2$ . Then  $k_i$  and  $k_d$  can be calculated explicitly

$$\begin{aligned} k_i(a) &= \frac{1}{2} \sqrt[3]{2\pi + 2\sqrt{16a^3 + \pi^2}} - 2 \frac{a}{\sqrt[3]{2\pi + 2\sqrt{16a^3 + \pi^2}}} \\ k_d(a) &= \frac{1}{2} \sqrt{-2a + 2\sqrt{a^2 + 4}}. \end{aligned} \quad (59)$$

It follows that for  $a < a_* \approx 0.2681736$ , where  $a_*$  is the solution of  $k_i(a_*) = k_d(a_*)$ , the consistency condition is violated and a significant contribution to the integral (57) has to come from the intermediate (bottleneck) range. We perform detailed numerical simulations to confirm this result. In Fig. (2) solutions of (49) are represented for  $a = 0, 1/4, 1/2, 1$  and a bottleneck is observed only for  $a = 1/4$  and  $a = 0$ . For  $a = 1$  there is clearly no bottleneck and there is practically no bottleneck in the case  $a = 1/2$  either.

We remark that for  $a \in (0, 2^{2/3}3)$ , that is for all values of  $a$  that we analyzed above, Eq. (52) has complex solutions. Thus, the corresponding solutions of Eq. (49) oscillate around  $\pm 1$  for  $X \rightarrow \pm\infty$ . But, as can be easily seen in Fig. (2) the amplitude of the oscillations decreases with increasing  $a$ . Thus, we view the oscillations appearing in the solutions when

$f(k)$  falls off too fast with  $k \rightarrow 0$  as another manifestation of the bottleneck phenomenon. The mere possibility of oscillations in solutions of Eq. (49) does not necessarily lead to a bump in the spectrum.

### 3.2. Perturbative expansion for the hyperviscous boundary-layer Burgers equation

A special case in which the bottleneck effect can be analyzed analytically is Eq. (49) with dissipation given by the function  $f(k) = k^{2\alpha}$ , when  $\alpha$  is close to unity. We write  $\alpha = 1 + \varepsilon$  and use  $\varepsilon$  as a small parameter. Noting that

$$k^{2\alpha} = k^2 k^{2\varepsilon} = k^2 \sum_{n=0}^{\infty} \frac{1}{n!} (2 \ln k)^n \varepsilon^n, \quad (60)$$

and assuming that  $u^{\text{in}}$  has an expansion in powers of  $\varepsilon$

$$u^{\text{in}} = \sum_{n=0}^{\infty} u^{(n)} \varepsilon^n, \quad (61)$$

with  $u^{(0)} = -\tanh \frac{x}{2}$  being the exact solution of Eq. (49) in the case  $f(k) = k^2$ , we obtain the following system of equations for the functions  $u^{(n)}$ ,  $n \geq 1$ : at the leading order  $n = 1$

$$(2 \ln \sqrt{-\partial_x^2})(-\partial_x^2)u_0 + (-\partial_x^2)u^{(1)} + u_0 \partial_x u^{(1)} + u^{(1)} \partial_x u_0 = 0, \quad (62)$$

and for  $n > 1$

$$(-\partial_x^2)u^{(n)} + u_0 \partial_x u^{(n)} + u^{(n)} \partial_x u_0 + \sum_{m=1}^n \frac{(2 \ln \sqrt{-\partial_x^2})^m}{m!} (-\partial_x^2)u^{(n-m)} + \sum_{m=1}^{n-1} u^{(m)} \partial_x u^{(n-m)} = 0. \quad (63)$$

Now we show that at every fixed  $n$ , in particular at  $n = 1$ , the function  $u^{(n)}$  can be explicitly written in terms of  $u^{(m)}$ , with  $0 \leq m < n$  and their Fourier transforms. Indeed, upon integrating the above equations we can rewrite them as

$$\partial_x u^{(n)} = u_0 u^{(n)} - g^{(n)}, \quad (64)$$

where, for  $n > 1$

$$g^{(n)} = \frac{2^n}{n!} \partial_x (\ln \sqrt{-\partial_x^2})^n u_0 + \sum_{m=1}^{n-1} \frac{2^m}{m!} \partial_x (\ln \sqrt{-\partial_x^2})^m u^{(n-m)} - \frac{1}{2} \sum_{m=1}^{n-1} u^{(m)} u^{(n-m)} \quad (65)$$

and

$$g^{(1)} = 2 \partial_x \ln \sqrt{-\partial_x^2} u_0, \quad (66)$$

for  $n = 1$ . Since for all  $n \geq 1$  functions  $u^{(n)}$  are odd, we can write the solutions of the linear inhomogeneous equations (64) as

$$u^{(n)}(x) = -\frac{1}{\cosh^2 \frac{x}{2}} \int_0^x g^{(n)}(x') \cosh^2 \frac{x'}{2} dx', \quad (67)$$

or, inserting the expressions for  $g^{(n)}$ , as

$$\begin{aligned} u^{(n)} = & - \sum_{m=1}^n \frac{2^m}{m!} \frac{1}{\cosh^2 \frac{x}{2}} \int_0^x \left( \partial_x (\ln \sqrt{-\partial_x^2})^m u^{(n-m)} \right) \cosh^2 \frac{x'}{2} dx' \\ & + \frac{1}{2} \sum_{m=1}^{n-1} \frac{1}{\cosh^2 \frac{x}{2}} \int_0^x u^{(m)} u^{(n-m)} \cosh^2 \frac{x'}{2} dx'. \end{aligned} \quad (68)$$

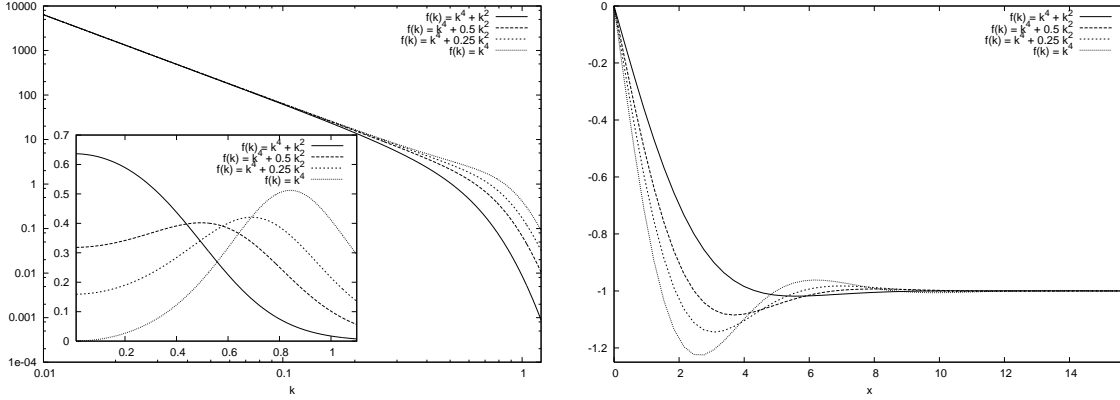


**Figure 2.** Numerical simulations of Eq. (49) with the dissipation term  $f(k) = k^4 + ak^2$ , with resolution  $N = 1024$  and domain size  $L = 400\pi$  for (a) and  $L = 100\pi$  for (b). In (a) we represent the spectrum of the inner solution  $|\hat{u}^{(\text{in})}|^2$  for  $a = 1$  (solid line),  $a = \frac{1}{2}$  (dashed line),  $a = \frac{1}{4}$  (dash-dotted line) and  $a = 0$  (dotted line). In the inset we represent  $f(k)|\hat{u}^{(\text{in})}|^2$  for different values of  $a$ :  $a = 1$  (solid line),  $a = \frac{1}{2}$  (dashed line),  $a = \frac{1}{4}$  (dash-dotted line) and  $a = 0$  (dotted line). In (b) we represent the solutions  $u^{(\text{in})}$  in the physical space for  $a = 1$  (solid line),  $a = \frac{1}{2}$  (dashed line),  $a = \frac{1}{4}$  (dash-dotted line) and  $a = 0$  (dotted line). The exponentially decaying oscillations around  $-1$  become stronger for smaller  $a$ .

Finally, by using explicit representation for the action of the pseudo-differential operators  $(\ln \sqrt{-\partial_x^2})^m$  we obtain the following expression for the function  $u^{(n)}$

$$u^{(n)} = \sum_{m=1}^n \frac{2^m}{m!} a_n^{(m)}(x) + \frac{1}{2} \sum_{m=1}^{n-1} b_n^{(m)}(x), \quad (69)$$

where

$$a_n^{(m)} = \frac{1}{\sqrt{2\pi}i} \left[ \int_{\mathbb{R}} \frac{k^2 (\ln |k|)^m}{1+k^2} (\mathcal{F}u^{(n-m)})(k) \sin kx \, dk + \frac{d}{dx} \tanh \frac{x}{2} \int_{\mathbb{R}} (\ln |k|)^m (\mathcal{F}u^{(n-m)})(k) \frac{\sin kx}{1+k^2} \, dk \right] \quad (70)$$

and

$$b_n^{(m)} = \frac{1}{\cosh^2 \frac{x}{2}} \int_0^x u^{(m)}(x') u^{(n-m)}(x') \cosh^2 \frac{x'}{2} \, dx'. \quad (71)$$

To study the bottleneck effect, it is enough to consider the first order term in Eq. (61), which gives

$$u^{(1)}(x) = 2 \int_{\mathbb{R}} \frac{k^2 \ln |k|}{\sinh(\pi k)} \frac{\sin kx}{1+k^2} \, dk + \frac{d}{dx} 2 \tanh \frac{x}{2} \int_{\mathbb{R}} \frac{\ln |k|}{\sinh(\pi k)} \frac{\sin kx}{1+k^2} \, dk \quad (72)$$

or, in the Fourier space,

$$(\mathcal{F}u^{(1)})(k) = \frac{2\sqrt{2\pi} k^2 \ln |k|}{i} \frac{1}{1+k^2} \frac{1}{\sinh \pi k} + \frac{2\sqrt{2\pi}}{i} k \int_{\mathbb{R}} \frac{1}{(k')^2 + 1} \frac{\ln |k'|}{\sinh \pi k'} \frac{1}{\sinh \pi(k-k')} \, dk',$$

where the integral has to be regularized in a suitable sense.

### 3.3. Truncated solutions

The arguments presented in the previous section imply that the best way to generate a bottleneck is to take for  $f(k)$  a function which vanishes for  $k$  smaller than a certain cut-off (which, without any loss of generality, we take to be 1) and is infinite for  $k$  above the cut-off

$$f_{\text{tr}}(k) = \begin{cases} 0 & \text{for } |k| < 1, \\ +\infty & \text{for } |k| > 1. \end{cases} \quad (73)$$

However, it is not clear how to implement such a dissipation term in Eq. (49). We approximate such a cut-off dissipation term by considering a function  $f(k)$  which depends on a certain parameter in such a way that when the parameter tends to infinity,  $f(k)$  tends to  $f_{\text{tr}}(k)$ . Here we consider two examples of such functions: (i) hyperviscosity  $f(k) = k^{2\alpha}$  in the limit  $\alpha \rightarrow \infty$ , a problem which has also been studied in [34] and (ii) a cosh-dissipation term exponentially growing for  $|k| \rightarrow \infty$

$$f(k) = e^{-\mu}(\cosh \mu k - 1), \quad (74)$$

introduced in [30] and studied further in [41]. Both functions tend to  $f_{\text{tr}}(k)$  for  $\alpha \rightarrow \infty$  and  $\mu \rightarrow \infty$  but behave differently in the dissipation range, as we have seen in Section 2.3.

For both types of dissipation we found that the solutions in the Fourier space seem to tend to a well-defined limit for  $|k| < 1$  and tend to zero for  $|k| > 1$ ; this is illustrated in Fig. (3). The latter observation follows immediately from Eq. (57). The former follows from the numerical results for the hyperviscous and the cosh-dissipation terms, with representative plots shown in Fig. (3), which also suggest that the limiting function, which we denote by  $u_\infty$ , does not depend on the precise form of  $f(k)$ . Numerically, the high  $\alpha$  and  $\mu$  solutions in the neighborhood of  $\pm 1$  are well described by the functional form

$$\hat{u}_\infty(k) = \begin{cases} a(1+k)^{-\Delta} + b, & -1 < k < 0, \quad k \sim -1, \\ -a(1-k)^{-\Delta} - b, & 0 < k < 1, \quad k \sim 1. \end{cases} \quad (75)$$

A good agreement of the numerical data with the functional form (75) is achieved for  $\Delta \approx 2/3$  and  $a \approx 0.2, b \approx 0.8$ .

Unfortunately, we did not manage to establish an equation for  $u_\infty$ , and thus, we do not have a theory which would explain the exponent  $\frac{2}{3}$  in its Fourier space representation. The main difficulty in establishing such an equation consists in determining the  $\alpha \rightarrow \infty$  or  $\mu \rightarrow \infty$  limit of the right hand side of Eq. (49) which we denote by  $R(u_\infty)$ . Clearly, whereas the support of the limiting function itself is  $\text{supp } u_\infty = [-1, 1]$ , the support of  $R(u_\infty)$  is contained in  $(-\infty, -1] \cup [1, +\infty)$ . More precisely, since on the left hand side of Eq. (49) we have a quadratic term, the support is equal to  $[-2, -1] \cup [1, 2]$ . Some information about  $R(u_\infty)$  can be obtained by using Eq. (55) for  $g(u) = \frac{1}{2}u|u|$  and  $G(u) = \text{sign}(u)$ , so that

$$\int_{\mathbb{R}} \text{sign}(u^{(\text{in})}) f \left( \sqrt{-\frac{d^2}{dX^2}} \right) u^{(\text{in})} dX = 1. \quad (76)$$



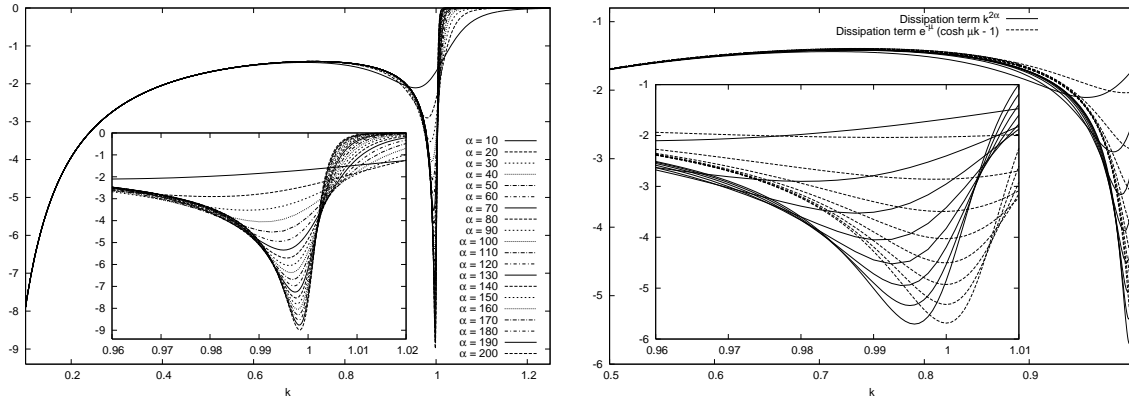


**Figure 3.** Numerical simulations of Eq. (49) with hyperviscous dissipation terms and cosh-dissipation terms. In (a) we represent solutions for hyperviscous dissipation terms with  $\alpha = 10, 20, \dots, 200$ . With increasing  $\alpha$  the solution tends to zero for  $k > 1$  and seems to acquire a well-defined limit for  $k < 1$ . In (b) we compare solutions for hyperviscous dissipation terms with  $\alpha = 10, 20, \dots, 80$  (solid lines) and cosh-dissipation terms with  $\mu = 20, 40, \dots, 160$  (dashed lines).

Based on numerical results we assume that  $\text{sign}(u^{(\text{in})}) = -\text{sign}(X)$ , which gives us the following relation for the term on the right hand side of Eq. (49)

$$\int_{\mathbb{R}} \text{sign}(X) f\left(\sqrt{-\frac{d^2}{dX^2}}\right) u^{(\text{in})}(X) dX = -1, \quad (77)$$

from which follows, via Parseval's theorem,

$$\int_{\mathbb{R}} \frac{f(k)}{k} \hat{u}^{(\text{in})}(k) dk = -i\sqrt{\frac{\pi}{2}}. \quad (78)$$

Relations (57) and (78), combined with numerical results, suggest that  $R(u_\infty)$  is a function and not a distribution. However, we did not succeed in determining the functional form of this function.

From the numerically obtained functional form of  $\hat{u}_\infty$  we deduce the asymptotic form of  $u_\infty$  in the physical space for  $X \rightarrow \infty$

$$u_\infty(X) \simeq \begin{cases} 1 + a\sqrt{\frac{2}{\pi}} \Gamma\left(\frac{1}{3}\right) (-X)^{-\frac{1}{3}} \sin\left(X + \frac{\pi}{6}\right) & \text{for } X \rightarrow -\infty, \\ -1 + a\sqrt{\frac{2}{\pi}} \Gamma\left(\frac{1}{3}\right) X^{-\frac{1}{3}} \sin\left(X - \frac{\pi}{6}\right) & \text{for } X \rightarrow +\infty. \end{cases} \quad (79)$$

#### 4. Spectrum of the one-dimensional Burgers equation with modified dissipation

In Sections 2 and 3 we have studied simplified models derived for solutions of the Burgers equation. Whereas the results of Section 2 concern dissipation scales only, Section 3 deals with the intermediate range between the inertial range and the dissipation range. In this section we shall see how far the results of the previous two sections can be used to analyze numerical solutions of the Burgers equation with modified dissipation in the Fourier space. We employ the following strategy: we solve the Burgers equation by using high-precision pseudo-spectral

simulations with the *mpfun*-package [43]. This approach allows us to analyze the solutions deep in the dissipation range which becomes the more important the faster the dissipation term grows with  $k$ . We employ the Exponential Time Differencing Runge-Kutta scheme [45, 44].

We concentrate essentially on the behavior of solutions in two ranges: the dissipation range (or the high wavenumber range) and the bottleneck range (or the transition range from the inertial to the dissipation range).

The functional form of solutions in the Fourier space in the dissipation range is studied by using the example of two different kinds of dissipation: the hyperviscous dissipation and the cosh-dissipation. Here we have the advantage that our numerical investigations of the  $|k| \rightarrow \infty$  asymptotics can be checked against the theoretical predictions of Eqns. (35) and (47). This is important in particular with regard to numerical studies of more general equations, such as the Navier–Stokes equations, for which analytical results concerning the form of the dissipation range are few.

To analyze the asymptotics in the dissipation range numerically, we apply the asymptotic extrapolation procedure of van der Hoeven [36]. This procedure can be viewed as a sequence of transformation techniques in which the main idea is to remove the higher leading-order terms by applying a suitable sequence of transformation and then, knowing the sub-leading order terms, to obtain the leading-order terms. The choice of the order and the type of transformations depends on the functional form of the analyzed sequence. In our case we essentially take the sequence used in [46] and [30].

For the hyperviscous dissipation term  $\nu^{2\alpha-1}k^{2\alpha}$  the dissipation range begins roughly at  $1/\nu$ . Taking  $\nu$  to be of order one gives us a solution which lies entirely in the dissipation range. For such a solution the small Reynolds number results of Section 2 apply in the first place and thus give us a means to check the validity of the small-Reynolds number expansion of Section 2. Unfortunately, numerical analysis in the case of  $\nu \sim 1$  turns out to be difficult, because for such values of  $\nu$  the solution in the Fourier space falls off very quickly, so that very high precision and extremely small time steps are required: the higher are the modes whose Fourier coefficients we calculate, the higher the precision and computational accuracy is needed.

As a consequence, in the expansion (35) only the leading and the two sub-leading terms can be reliably determined. For example, the exponent of the algebraic prefactor is obtained with a relative precision of order  $10^{-4}$  whereas for the rate of exponential decay we get a precision of  $10^{-7}$  as shown in Fig. (4). We did not succeed in determining any further sub-leading terms, such as complex powers of  $k$ , because of several reasons related to insufficiently small time steps and a lack of sufficient number of modes for extrapolation.

Simulations employing cosh-dissipation give results similar to the hyperviscous case. Hence for the dissipation term  $f(k) = (\cosh k - 1)$  the leading-order term  $\exp(-Ck \ln k)$  can be clearly identified. In particular, the numerical value of the constant  $C = -1/\ln 2$  conjectured in [30] and predicted by Eq. (47) can be confirmed with certainty as shown in Fig. (4b). Unfortunately, the determination of higher order term in the asymptotic expansion is hampered by the logarithmic-scale oscillations present in the next-order correction  $\exp(kg(\ln k))$  (function  $g(\cdot)$  is periodic with period  $\ln 2$ ) giving rise to the logarithmic scale

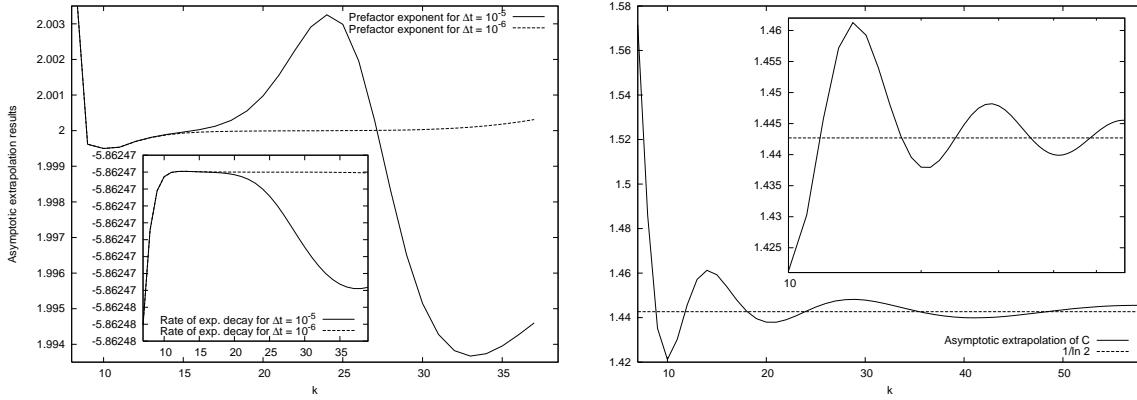


**Figure 4.** (a) Results of asymptotic extrapolation procedure applied to the Fourier coefficients of the solution of Eq. (2) with  $\nu = 1$  and  $\alpha = 2$ , initial condition  $\sin x$ , calculated with 200 digits and time step  $10^{-6}$ . At the fourth stage of asymptotic extrapolation the sequence tends to the constant value  $-2/\alpha$ . The deviations from this value is of the order  $10^{-4}$ .

oscillations in Fig. (4b).

What happens when the dissipation term starts acting at wavenumbers much higher than one, so that a substantial inertial range can be developed? As we shall see now, although the functional form predicted by the small Reynolds number expansion can be identified in the dissipation range, for dissipation terms producing large bottlenecks this becomes increasingly difficult, since one has to go to higher and higher wavenumbers to recover the asymptotic behavior of the Fourier coefficients of solutions. At the same time the parts of the bottleneck region adjacent to the inertial range are satisfactorily described by the linear asymptotic approximation based on Eq. (54).

We have calculated solutions of the Burgers equation with hyperviscous dissipation terms of the type  $\nu^{2\alpha-1}k^{2\alpha}$  for small  $\nu$  numerically by using high-precision for several values of  $\alpha$ . For  $\alpha = 2$  the functional form of the dissipation range is identified quite accurately: For example, for the numerical solution using  $\nu^3 = 10^{-8}$ , the exponent of the algebraic prefactor is determined with the relative precision of the order  $10^{-2}$ , for the rate of exponential decay the relative precision is of the order  $10^{-5}$  as shown in Fig. (5). Remarkably, to obtain the functional form of the solution in the dissipation range accurately even for  $\alpha = 2$  we have to go quite far beyond the wavenumber  $1/\nu \approx 464$ , i.e. the wavenumber at which dissipation sets in. For example, as can be seen in Figure 5, the relative error in the determination of the prefactor exponent drops below  $10^{-2}$  only for  $k > 5/\nu \approx 2321$ . For  $\alpha = 3$  and  $\nu^5 = 10^{-14}$  we would have to go even farther beyond the wavenumber  $1/\nu^{1/5} \approx 631$ : for  $k > 5/\nu^{1/5} \approx 3155$  and up to  $N/2 = 10^{12}$  the asymptotic extrapolation procedure for the algebraic prefactor exponent does not converge to any value, displaying oscillations similar to those in Fig. (5a), but much stronger. For the rate of exponential decay the error is of the order  $10^{-4}$  if we assume that the algebraic prefactor is  $k^4$ . Even worse convergence to asymptotic behavior is observed for the exponentially growing dissipation terms for which even the identification of the leading order term requires resolutions much higher than  $1/\nu$ .

For the bottleneck region we use the results of Section 3.1, in particular the numerical

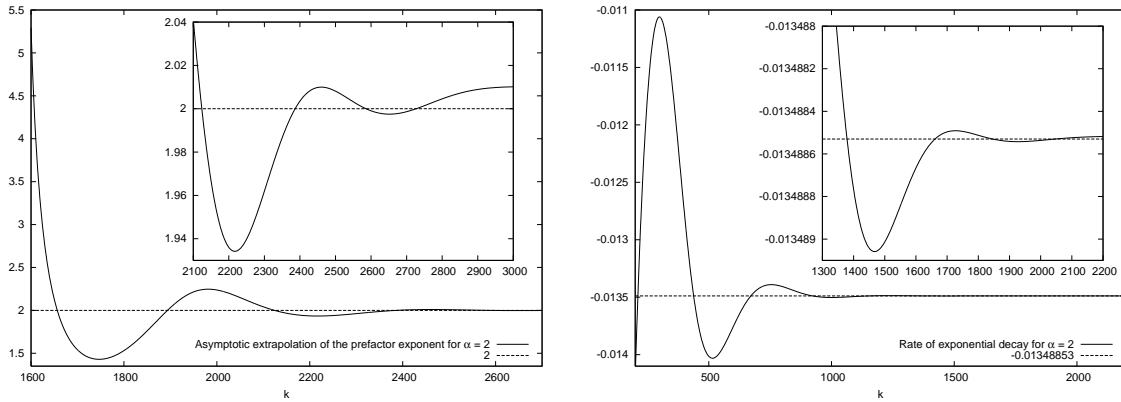


**Figure 5.** Results of asymptotic extrapolation procedure applied to Fourier coefficients of the solution of Eq. (2) with  $\nu = 10^{-8}$  and  $\alpha = 2$ , initial condition  $\sin x$ , calculated with 54 digits, time step  $\Delta t = 10^{-5}$  and resolution  $N = 2^{13}$  at time  $t = 1.1$ . Panel (a) are the results for the algebraic prefactor exponent for which the analytical value is  $2\alpha - 2 = 2$ . The deviations from the theoretical value are of order  $10^{-2}$  for wavenumbers between 2400 and 2800. Panel (b) shows the results of asymptotic extrapolation for the rate of exponential decay in the leading-order term.

values of the amplitude  $A$  and of the phase shift  $\phi$ . The functional form of solutions in the bottleneck region (Eq. (54)) is approximated by the linearized asymptotic solution  $\hat{u}_{as}^{(in)}(k)$  of the boundary layer Burgers equation (49) as

$$\hat{u}(k) \simeq \frac{1}{\sqrt{2\pi}} \frac{J}{k_e} \hat{u}_{as}^{(in)}(k/k_e), \quad (80)$$

where  $J$  is the jump in the entropic solution at the shock, by Fast-Legendre transforms, and  $k_e = 2^{\alpha-1} \sqrt{J}/\nu$  is the effective dissipation wavenumber. As can be seen in Fig. (6) on the example of the hyperviscous Burgers equation with  $\alpha = 2$  and  $\nu^3 = 10^{-8}$ , the agreement of the approximative solution with the actual solution is extremely good.

## 5. Conclusions

In this article we have seen by using the example of the one-dimensional Burgers equation with a modified dissipation term how the structure of solutions of a hydrodynamical equation can be described by simplified models which can be obtained from the original equation by systematic reduction. We have concentrated on the far dissipation region and the transition region from the inertial range to the dissipation range.

To study the far dissipation region we have presented a method which allows us to study solutions of hydrodynamical equations at small Reynolds numbers in domains with periodic initial conditions. This method takes advantage of the fact that for initial conditions with suitably restricted modes the interaction between modes is restricted and solutions can be obtained recursively without any errors due to truncation or time-stepping. It is applicable to more general hydrodynamical equations such as the Navier–Stokes equations which was one of the reasons to present it here. For the one-dimensional Burgers equation in the limit

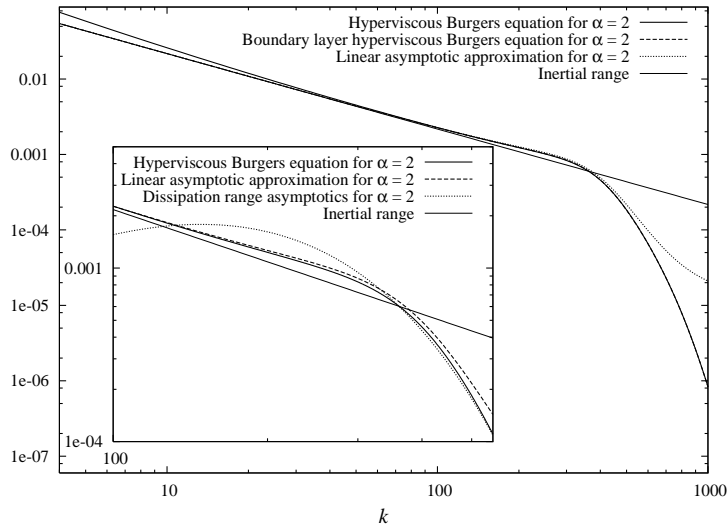


**Figure 6.** Log-log scale representation of the Fourier coefficients of the solution of Eq. (2) with  $\nu = 10^{-8}$  and  $\alpha = 2$ , initial condition  $\sin x$ , calculated with 54 digits, time step  $\Delta t = 10^{-5}$  and resolution  $N = 2^{13}$  at time  $t = 1.1$ . We compare this solution with the solution of the boundary layer Burgers equation, the rescaled linearized asymptotic solution and the inertial range scaling  $\sim k^{-1}$ . In the inset the numerical solution of Eq. (2) is compared with the functional form in the dissipation range, the rescaled linearized asymptotic solution and the inertial range scaling.

of long times the problem can be simplified even further, so that the problem reduces to a non-linear difference-differential equation. By using this equation we have studied the high wavenumber asymptotics in detail and verified the results by using high-precision pseudo-spectral numerical simulations.

We have seen that the transition range from the inertial range to the dissipation range in the case of the Burgers equation can be described quite well by a linearized solution of the boundary layer problem in the neighborhood of shocks. However, in contrast to the study of the far dissipation range where the analysis has been done by a method which a priori does not use any special properties of the one-dimensional Burgers equation, in the study of the intermediate range we had to rely on a very special property of the Burgers equation. A further drawback is that we were not able to determine analytically the amplitude and the phase of oscillations near the shocks and had to use numerics to determine them.

How far the analysis presented in this article is applicable to the Navier–Stokes equations? As we stated above, the method for the analysis of the far dissipation range presented here can be extended to the Navier–Stokes equations in arbitrary dimensions. The main difference to the Burgers case is that the corresponding recursion relations are hard to deal with analytically and have to be studied numerically using high-precision arithmetics, analogously to singularities of the Euler equation [48, 49, 50]. The results of this ongoing work will be published elsewhere.

The treatment of the bottleneck problem seems to be more difficult because the Burgers type analysis does not apply to incompressible flows. It is known that the bump in the energy

spectrum appears together with oscillations in the physical space [27, 26], but we are still far from understanding this phenomenon analytically.

We thank D. Banerjee for several useful discussions and collaborations; we also thank D. Vincenzi for encouragement. SSR acknowledges DST (India) project ECR/2015/000361 for financial support.

- [1] L. D. Landau and E. M. Lifshitz, *Fluid Mechanics* (Pergamon Press, 1987), Volume 6 of Course of Theoretical Physics, Second English Edition, Revised.
- [2] U. Frisch, *Turbulence: The Legacy of A.N. Kolmogorov* (Cambridge University, Cambridge, UK, 1996).
- [3] A.N. Kolmogorov, Dokl. Akad. Nauk SSSR **30**, 301 (1941); A.N. Kolmogorov, Dokl. Akad. Nauk SSSR **31**, 538 (1941).
- [4] G. Falkovich, K. Gawedzki and M. Vergassola, Rev. Mod. Phys. **73**, 913 (2001).
- [5] R. Pandit, P. Perlekar, and S.S. Ray, Pramana **73**, 157 (2009).
- [6] C. Fefferman, *Existence and smoothness of the Navier-Stokes equation. Clay Millennium Prize Problem Description* (2000); [http://www.claymath.org/millennium/Navier-Stokes\\_Equations/Official\\_Problem\\_Description.pdf](http://www.claymath.org/millennium/Navier-Stokes_Equations/Official_Problem_Description.pdf).
- [7] G. Eyink, U. Frisch, R. Moreau, and A. Sobolevskii, Proceedings of *Euler Equations: 250 Years On*, Aussois, June 18–23, 2007; *Physica D* **237** (2008)
- [8] A. J. Majda and A. L. Bertozzi, *Vorticity and Incompressible Flow*. Cambridge Texts in Applied Mathematics, Cambridge University Press, Cambridge (2001).
- [9] U. Frisch, T. Matsumoto, and J. Bec, J. Stat. Phys. **113** 761 (2003).
- [10] C. Bardos, E. S. Titi, Uspekhi Mat. Nauk **62**(2007), 5 (2007) [English version: Russian Math. Surv. **62** 409 (2007).]
- [11] P. Constantin, Bull. Amer. Math. Soc. **44** 603 (2007).
- [12] J. L. Lions, *Quelques Méthodes de Résolution des Problèmes aux Limites non Linéaires*, Gauthier-Villars, Paris (1969).
- [13] P. Constantin and C. Foias, *Navier-Stokes equations*. Chicago Lectures in Mathematics. University of Chicago Press, Chicago, (1988).
- [14] R. Temam, *Navier-Stokes equations. Theory and numerical analysis*. Revised edition. With an appendix by F. Thomasset. Published by AMS Bookstore (2001).
- [15] H. Sohr *The Navier-Stokes equations*, Birkhäuser, Basel (2001).
- [16] J. Bec and K. Khanin, Phys. Reports **447**, 1 (2007).
- [17] J. von Neumann, in *Collected Works (1949–1963), Vol. 6, 1949*, edited by A. H. Taub (Pergamon Press, New York, 1963), p. 437.
- [18] C. Foias, O. Manley and L. Sirovich, Phys. Fluid A **2**, 464 (1990).
- [19] S. Chen, G. Doolen, J. R. Herring, R. H. Kraichnan, S. A. Orszag and Z. S. She, Phys. Rev. Lett. **70**, 3051 (1993).
- [20] D. O. Martínez, S. Chen, G. D. Doolen, R. H. Kraichnan, L.-P. Wang, and Y. Zhou, J. Plasma Phys. **57**, 195 (1997).
- [21] R. H. Kraichnan, J. Fluid Mech. **5**, 497 (1959).
- [22] Y. Kaneda, T. Ishihara, M. Yokokawa, K. Itakura, and A. Uno, Phys. Fluids **15**, L21 (2003).
- [23] G. Falkovich, Phys. Fluids **6**, 1411 (1994).
- [24] A. G. Lamorgese, D. A. Caughey, and S. B. Pope, Phys. Fluids **17**, 015106 (2005).
- [25] U. Frisch, S. Kurien, R. Pandit, W. Pauls, S. S. Ray, A. Wirth, and J-Z Zhu, Phys. Rev. Lett. **101**, 144501 (2008).
- [26] U. Frisch, S. S. Ray, G. Sahoo, D. Banerjee, and R. Pandit, Phys. Rev. Lett. **110**, 064501 (2013)
- [27] D. Banerjee and S. S. Ray, Phys. Rev. E **90**, 041001(R) (2014).
- [28] S. S. Ray, Pramana - Journal of Physics, **84**, 395 (2015).
- [29] O. A. Ladyzhenskaya, *The Mathematical Theory of Viscous Incompressible Flow* (1st ed.) Gordon and Breach, New York (1963).

- [30] C. Bardos, U. Frisch, W. Pauls, S. S. Ray and E. Titi, *Comm. Math. Phys.* 293(2), 519 (2010).
- [31] J. M. Burgers, *Adv. in Appl. Mech.* **1**, 171 (1948).
- [32] U. Frisch and J. Bec, in *Les Houches 2000: New Trends in Turbulence, Springer EDP Science, 2001*, edited by M. Lesieur, A. Yaglom and F. David (Les Houches Session LXXIV 31 July - 1 September 2000).
- [33] G. Falkovich, in *Non-equilibrium Statistical Mechanics and Turbulence*, edited by S. Nazarenko and O. V. Zaboronski (London Mathematical Society Lecture Note Series, 2008).
- [34] J. P. Boyd, *J. Sci. Comput.* 9, 81 (1994).
- [35] K. Yosida, *Functional Analysis*, Springer-Verlag Berlin Heidelberg (1995).
- [36] J. van der Hoeven, *J. Symb. Comput.* 44(8), 1000 (2009).
- [37] W. Pauls, in preparation.
- [38] G. E. Andrews, *The Theory of Partitions* (Cambridge University Press, 1984).
- [39] B. Ya. Levin, *Lectures on Entire Functions* (American Mathematical Society, 1996).
- [40] J. P. Boyd, *J. Atmos. Sci.* 49, 128 (1992).
- [41] J.-Zh. Zhu and M. Taylor, *Chinese Phys. Lett.* 27, 054702 (2010).
- [42] J. P. Boyd, *Chebyshev and Fourier Spectral Methods* (Dover, 2001).
- [43] D. H. Bailey, *ACM Transactions on Mathematical Software* 21, 379 (1995).
- [44] S. M. Cox and P. C. Matthews, *J. Comput. Phys.* 176, 430 (2002).
- [45] A.-K. Kassam and L. N. Trefethen, *SIAM J. Sci. Comput.* 26, 1214 (2005).
- [46] W. Pauls and U. Frisch, *J. Stat. Phys.* 127, 1095 (2007).
- [47] S. Chakraborty, U. Frisch and S. S. Ray, *J. Fluid Mech.* 649, 275 (2010).
- [48] T. Matsumoto, J. Bec, U. Frisch, *Fluid Dynam. Re.* 36, 221 (2005).
- [49] W. Pauls, T. Matsumoto, U. Frisch, J. Bec, *Physica D* 219, 4059 (2006).
- [50] W. Pauls, *Physica D* 239, 1159 (2010).